Ultrasound-derived Biceps Femoris Long-Head Fascicle Length: Extrapolation Pitfalls

Franchi, Martino V ; Fitze, Daniel P ; Raiteri, Brent J ; Hahn, Daniel ; Spörri, Jörg

Abstract: PURPOSE To compare biceps femoris long-head (BFlh) fascicle lengths (Lfs) obtained with different ultrasound-based approaches: 1) single ultrasound images and linear Lf extrapolation; 2) single ultrasound images and one of two different trigonometric equations (termed equations A and B); and 3) extended field of view (EFOV) ultrasound images. METHODS Thirty-seven elite alpine skiers (21.7±2.8 yrs) without a previous history of hamstring strain injury were tested. Single ultrasound images were collected with a 5 cm linear transducer from BFlh at 50% femur length and were compared with whole muscle scans acquired by EFOV ultrasound. RESULTS The intra-session reliability (ICC3,k = intra-class correlation coefficient) of Lf measurements was very high for both single ultrasound images (i.e., Lf estimated by linear extrapolation; ICC3,k = 0.96-0.99, SEM = 0.18 cm) and EFOV scans (ICC3,k = 0.91 -0.98, SEM = 0.19 cm). Although extrapolation methods showed cases of overestimation and underestimation of Lf when compared with EFOV scans, mean Lf measured from EFOV scans (8.07±1.36 cm) was significantly shorter than Lf estimated by trigonometric equations A (9.98±2.12 cm, P<0.01) and B (8.57±1.59 cm, P=0.03), but not significantly different from Lf estimated with manual linear extrapolation (MLE) (8.40±1.68 cm, p=0.13). Bland-Altman analyses revealed mean differences in Lfs obtained from EFOV scans and those estimated from equation A, equation B and MLE of 1.91±2.1 cm, 0.50±1.0 cm and 0.33±1.0 cm, respectively. CONCLUSIONS The typical extrapolation methods used for estimating Lf from single ultrasound images are reliable within the same session, but not accurate for estimating BFlh Lf at rest with a 5-cm FOV. We recommend that EFOV scans are implemented to accurately determine intervention-related Lf changes in BFlh.

DOI: https://doi.org/10.1249/MSS.0000000000002123

Medicine & Science IN Sports & Exercise
The Official Journal of the American College of Sports Medicine
www.acsm-msse.org

. . . Published ahead of Print

Ultrasound-derived Biceps Femoris Long-Head Fascicle Length: Extrapolation Pitfalls

Martino V Franchi[1, 2], Daniel P Fitze[2], Brent J Raiteri[3], Daniel Hahn[3,4], and Jörg Spörri[2]

[1]Institute of Physiology, Department of Biomedical Sciences, University of Padua, Italy; [2]Sports Medical Research Group, Department of Orthopaedics, Balgrist University Hospital, University of Zurich, Switzerland; [3]Ruhr University Bochum, Faculty of Sports Science, Human Movement Science, Germany; [4]School of Human Movement and Nutrition Sciences, University of Queensland, Brisbane, Australia

Accepted for Publication: 26 July 2019

Medicine & Science in Sports & Exercise, Publish Ahead of Print
DOI: 10.1249/MSS.0000000000002123

Ultrasound-derived Biceps Femoris Long-Head Fascicle Length: Extrapolation Pitfalls

Martino V Franchi[1, 2], Daniel P Fitze[2], Brent J Raiteri[3], Daniel Hahn[3,4], and Jörg Spörri[2]

[1]Institute of Physiology, Department of Biomedical Sciences, University of Padua, Italy

[2]Sports Medical Research Group, Department of Orthopaedics, Balgrist University Hospital, University of Zurich, Switzerland

[3]Ruhr University Bochum, Faculty of Sports Science, Human Movement Science, Germany

[4]School of Human Movement and Nutrition Sciences, University of Queensland, Brisbane, Australia

Address for correspondence:

Dr Martino Franchi

Institute of Physiology,

Department of Biomedical Sciences,

University of Padua, Italy

martino.franchi@unipd.it

The authors would like to thank Swiss Ski and Balgrist foundation stitftung for the financial support for the present study. The authors declare the non-presence of any conflict of interests. The results of the present study do not constitute endorsement by ACSM. The results of the present study are presented clearly, honestly, without fabrication, falsification or inappropriate data manipulation.

Abstract

Purpose: To compare biceps femoris long-head (BFlh) fascicle lengths (Lfs) obtained with different ultrasound-based approaches: 1) single ultrasound images and linear Lf extrapolation; 2) single ultrasound images and one of two different trigonometric equations (termed equations A and B); and 3) extended field of view (EFOV) ultrasound images. **Methods:** Thirty-seven elite alpine skiers (21.7±2.8 yrs) without a previous history of hamstring strain injury were tested. Single ultrasound images were collected with a 5 cm linear transducer from BFlh at 50% femur length and were compared with whole muscle scans acquired by EFOV ultrasound. **Results:** The intra-session reliability ($ICC_{3,k}$ = intra-class correlation coefficient) of Lf measurements was very high for both single ultrasound images (i.e., Lf estimated by linear extrapolation; $ICC_{3,k}$ = 0.96-0.99, SEM = 0.18 cm) and EFOV scans ($ICC_{3,k}$ = 0.91 -0.98, SEM = 0.19 cm). Although extrapolation methods showed cases of overestimation and underestimation of Lf when compared with EFOV scans, mean Lf measured from EFOV scans (8.07±1.36 cm) was significantly shorter than Lf estimated by trigonometric equations A (9.98±2.12 cm, P<0.01) and B (8.57±1.59 cm, P=0.03), but not significantly different from Lf estimated with manual linear extrapolation (MLE) (8.40±1.68 cm, p=0.13). Bland-Altman analyses revealed mean differences in Lfs obtained from EFOV scans and those estimated from equation A, equation B and MLE of 1.91±2.1 cm, 0.50±1.0 cm and 0.33±1.0 cm, respectively. **Conclusions:** The typical extrapolation methods used for estimating Lf from single ultrasound images are reliable within the same session, but not accurate for estimating BFlh Lf at rest with a 5-cm FOV. We recommend that EFOV scans are implemented to accurately determine intervention-related Lf changes in BFlh. **Keywords:** muscle architecture; ultrasound imaging; hamstrings; injury prevention, pennation angle, panoramic ultrasound

Introduction

Hamstring muscle strain injuries represent the most frequent injuries in running-based sports (1). Of the hamstring muscles, the biceps femoris long head (BFlh) has the highest risk for both injury and reinjury (1–3). Thus, it is unsurprising that the mechanics of this muscle during running (and especially sprinting) are of major interest. Due to difficulties of imaging the BFlh during high-speed movements *in vivo*, the first evidence of its fibre strains during sprinting have been derived from finite-element musculoskeletal simulations, whereby peak local fibre strains and fibre strain non-uniformities were shown to increase with faster running speeds (4). As BFlh injuries frequently may occur in the late swing phase of sprinting (i.e., at long muscle lengths where the hip is flexed) (3), when its muscle-tendon unit is undergoing active lengthening, it has been suggested that relatively longer muscle fibres may reduce the risk of injury during this phase. As long compared with short muscle fibres are assumed to reflect more sarcomeres in series, the proposed mechanism is that during fast eccentric actions (i. e., rapid fibre stretch during active muscle-tendon lengthening), longer muscle fibres will exhibit less strain per sarcomere for a given muscle-tendon unit strain and stiffness (5).

In order to examine the relationship between BFlh fascicle length (Lf) and injury risk over the duration of a sport season, recent studies have primarily used B-mode ultrasound imaging to examine BFlh muscle architecture at rest (under the assumption that Lf is reflective of total fibre length and the number of sarcomeres in series). Indeed, short BFlh Lfs were found to be a strong indicator of relative injury risk (i.e., shorter Lf than 10.6 cm resulted in 4.1 greater risk of hamstring strain injury) (1). However, a major problem with previous BFlh Lf estimates is that they have been derived from linear extrapolation methods that assume no fascicle or aponeurosis

curvature exists and that muscle architecture is homogenous throughout the muscle. This is concerning given that the visible portions of the BFlh fascicles are often ~30-50% of their total resting length with a conventional image region of interest (ROI) of 4-5 cm (6, 7), which requires an extrapolation of at least 50%. Although Ando and colleagues have shown that some specific linear extrapolation methods can be valid for estimating Lf of vastus lateralis and intermedius (8), similar methods (trigonometric estimations) have been found to be unacceptable for the vastus medialis muscle, which presents regionally varying and substantial fascicle curvature (9). Regardless, the three most common extrapolation methods for assessing BFlh Lf from single ultrasound images include: 1) a manual linear extrapolation method (MLE), which has been described by Potier et al. (10) and consists of extrapolating visible fascicles with straight lines over the non-visible portion of the muscle up to the intersection point with the linearly-projected superficial aponeurosis of the muscle (Fig. 1); 2) a trigonometric equation that provides estimations of Lf based on linear extrapolation of a straight line parallel with a visible portion of a fascicle, which has proven suitable for estimating VL and vastus intermedius Lfs (8) and was put forward by Blazevich and colleagues (9) (this will be referred to as "equation A" from this point forward), and; 3) a second trigonometric equation as described by Finni and colleagues (11), in which only the non-visible portion of the fascicle (i.e., outside the FOV) is linearly extrapolated (this will be termed "equation B").

A potential method for accurately determining BFlh Lf *in vivo* may be the extended field of view (EFOV) ultrasound technique, which can provide panoramic images of the whole muscle, to allow Lf to be directly assessed without any extrapolation required (12). In fact, a few studies have already adopted EFOV to investigate BFlh muscle architecture (7, 13, 14) (15). Recently,

Pimenta and colleagues (7) showed that Lf extrapolation (using equation B) from single ultrasound images resulted in an average absolute error of between 0.74 to 0.93 cm in Lf estimation compared with the EFOV technique, despite between-session ICCs for each method ranging from 0.86-0.95. However, to date, no study has directly compared the accuracy of Lf estimates obtained from a range of linear extrapolation methods to the Lfs obtained from EFOV ultrasound imaging. This is a necessary comparison to provide confidence in the accuracy of BFlh Lf estimates and to understand whether any under- or overestimations in Lf from different extrapolation methods are likely to be systematic or random so that meaningful intervention-related changes in Lf can be determined. The aim of the present study was thus to compare BFlh Lf estimates obtained from the three most commonly used extrapolation methods with the Lfs measured from EFOV scans in a cohort of elite athletes. We hypothesized that estimates of Lf from three standard linear extrapolation methods of the same visible fascicles would be different to the Lfs determined with EFOV ultrasound imaging.

Methods

Participants

Thirty-seven elite alpine skiers (17 females and 20 males, 21.7±2.8 yrs) participated in this study. This study was approved by the institutional review board and the local ethics committee (KEK-ZH-NR: 2017-01395) and written informed consent was freely given by all subjects prior to participation.

Ultrasound imaging

Ultrasound images were acquired with an ultrasound device (Aixplorer Ultimate, SuperSonic Imagine, Aix-en-Provence, France) using a linear 5 cm transducer with an imaging depth of 5 cm (SuperLinear SL18-5, SuperSonic Imagine, Aix-en-Provence, France). Participants were instructed to rest in a prone position with their knees extended, with their feet laying off the bed for comfort and they were instructed to remain relaxed during image acquisition. For the single ultrasound images, the ROI was determined as follows. Firstly, 50% of femur length was marked as the distance between the greater trochanter and the mid-patella point. At 50% of femur length, the medial and lateral borders of the BFlh were then identified with ultrasound imaging. The ultrasound transducer was then positioned at 50% of femur length at the mid-distance between the BFlh's medial and lateral muscle borders. The transducer was then aligned to the fascicle plane, which was assumed to correspond to the image with the most continuous and visible muscle fascicles while the superficial and intermediate aponeuroses remained parallel (FIG 1 B). For the EFOV scan, the proximal (i.e., conjoint tendon of the BFlh and semitendinosus muscles) and distal musculo-tendinous junctions were firstly located and then the path of the BFlh was pre-determined (i.e., drawn on the skin as shown in Fig 1) by following its fascicles in the superficial compartment proximo-distally while trying to manipulate the transducer so that the fascicles remained continuous and visible and the aponeuroses remained parallel. The best ultrasound imaging path was then marked along the longitudinal plane (FIG 1 A). For the acquisition of the EFOV images, the transducer was moved slowly and continuously along the marked path with a constant pressure from the distal to the proximal musculo-tendinous junctions while transducer orientation was continuously adjusted as described above in order to stay in the fascicle plane (7). During the scans, in order to keep the ultrasound beam

perpendicular to the aponeurosis, the orientation of the transducer was slightly adjusted between the distal region of the muscle (approximately 20-25% of femur length) and the start of the mid-muscle belly (approximately 30-35% of femur length), where a change in fascicle arrangement was seen along the BFlh muscle belly. This point was pre-determined by the operator (MVF) and marked on the skin as a reference for the successive image acquisitions. For all scans, transmission gel was used to improve the acoustic contact and to keep the transducer pressure on the skin to a minimum.

Muscle (BFlh) architecture assessment

Lf, pennation angle (PA) and muscle thickness (MT) were digitized using an image-processing program (ImageJ 1.48v, National Institutes of Health, Bethesda, USA). For the single ultrasound images, the superficial aponeurosis was extended linearly towards the distal portion of the muscle using the straight-line tool in ImageJ software. The primary inclusion criterion for ultrasound image analyses was that the aponeuroses were parallel as the angle between the superficial and intermediate aponeuroses can strongly influence the extrapolation methodologies (6, 9). Thus, images that presented an angle between aponeuroses of greater than 4° were excluded from the analyses of Lf. For this reason, a total of 22 athletes – 9 females and 13 males - were included for Lf assessment and subsequent methodology comparisons (i.e., the data presented for PA and MT refer to the total number of subjects, n=37).

The inclusion criteria for determining appropriate fascicles to analyze were the following: the fascicle insertion point into the intermediate aponeurosis must have been clearly visible and a reasonable portion of the fascicle (~25% or more of the total estimated length) must have been

visible within the ultrasound transducer's field of view. Four fascicles that met such criteria in each image were drawn using the segmented line tool in ImageJ. The estimation of the Lf was carried out using the three different methods described below: (i) *manual linear extrapolation*, (ii) *equation A* and (iii) *equation B*. For MLE, the visible portion of a fascicle was outlined using the segmented line tool and was extrapolated linearly to the linearly projected line of the superficial aponeurosis (10).

In the second method, Lf was calculated using trigonometric equation A (9):

$$Lf = \sin(\gamma + 90°) \times MT / \sin(180° - (\gamma + 180° - \theta))$$

where γ was the angle between the superficial and intermediate aponeurosis, MT was the averaged muscle thickness and θ was the pennation angle in degrees.

In the third method, Lf was calculated using trigonometric equation B (11):

$$Lf = L + (h / sin\beta)$$

where L was the visible Lf from the intermediate aponeurosis to the most visible distal endpoint within the field of view (measured by following the non-linear path of the fascicle, and thus, for the present paper, accounting for the curvature of the visible portion of fascicles), h was the distance between the superficial aponeurosis and the most visible distal endpoint of the fascicle

and β was the angle, in degrees, between the linearly extrapolated fascicle and the linearly extended superficial aponeurosis.

For the EFOV ultrasound image analysis, the field of view of the single ultrasound image was first identified using pre-determined knowledge of the distance between 50% of femur length and the most distal insertion point of the muscle (assessed before scan acquisition through ultrasound image inspection) and by recognition of fat tissue distribution similarities, as well as by double checking the ROI by measuring the values of muscle thickness of BFlh and biceps femoris short-head in both static ultrasound and EFOV (Fig 1 C). Subsequently, as above, four fascicles from the same region as in the single ultrasound images were considered for analyses. The Lf was considered as the fascicle running from the intermediate to the superficial aponeuroses and was directly evaluated by using the segmented line tool, which allowed fascicle and superficial aponeurosis curvature to be taken into account.

PA was measured as the angle between the drawn fascicle and the intermediate aponeuroses. MT was measured as the distance between the superficial and intermediate aponeuroses using the straight-line tool. Within the ROI, MT was measured five times (proximo-distally) and the average MT values were calculated.

In EFOV scans only, architecture for the distal muscle site was assessed. The fascicles that were considered for evaluation were the ones that presented their insertion into the intermediate aponeuroses outside of the previously-defined ROI for mid-muscle belly architecture assessment.

Test-retest repeatability

In a restricted cohort of 6 volunteers, test-retest reliability for both ultrasound techniques (i.e., single snapshot vs. EFOV) was assessed by calculating the intraclass correlation coefficient ($ICC_{3,k}$) and the Pearson's correlation coefficient (r) for all muscle architecture parameters as described in Pimenta et al. (9). A high intra-day repeatability was classified as 0.70-0.90 and very high as >0.90. Standard error of measurement (SEM) was also calculated for every parameter. Both EFOV and single ultrasound images were acquired twice after completely removing the transducer from the skin and with 5 min rest between image acquisitions.

Comparison between the different techniques

Normality of Lf, PA and MT data was determined using the Shapiro-Wilk test. One-way repeated measures ANOVAs were performed in order to identify differences between techniques (EFOV, linear extrapolation, equation A, and equation B) on calculated or measured Lf values analyzed from EFOV scans or single ultrasound images. Bonferroni post-hoc tests were performed to determine the methods that were significantly different from each other. To determine differences in PA and MT between the single ultrasound images and EFOV images, paired t-tests were utilized. The family-wise type I error rate was set at 0.05.

For Lf, Pearson's correlation coefficients were calculated between values obtained by EFOV and each extrapolation method. For PA and MT values, Pearson's correlation coefficients were calculated between values obtained by EFOV and single ultrasound images. The agreement between Lfs calculated from each extrapolation method to those determined from EFOV images was assessed with Bland-Altman analysis. The average absolute error was determined for Lf

between EFOV, LE, equation A and equation B, whereas the average absolute error was only assessed between EFOV scans vs. single snapshot images for PA and MT. Pearson's correlation coefficient was calculated for all muscle architecture parameters, according to the design by Pimenta and colleagues (9). Pearson's coefficients were classified as weak (<0.3), moderate (0.3-0.7) and strong (>0.7).

Results

Test-retest repeatability

The intra-session reliability data ($ICCs_{3,k}$, Pearson's correlations and SEMs) for the muscle architecture parameters of interest from the EFOV scans and single ultrasound images are presented in Table 1. For Lf evaluation, both single ultrasound images (MLE) and EFOV scans showed a very high reliability ($ICC_{3,k}$ 95%CI: 0.96-0.99 and 0.91-0.98, SEM: 0.18 and 0.19, respectively). A very high repeatability was also observed for MT measurements from both ultrasound techniques ($ICC_{3,k}$ 95%CI: 0.92-0.98 and 0.88-0.97, SEM: 0.04 and 0.04 for single and EFOV images, respectively), whereas PA showed only high relative reliability ($ICC_{3,k}$ 95%CI: 0.69-0.93 and 0.73-0.95, SEM: 0.5 and 0.34 for single and EFOV images, respectively).

Extrapolation methods comparisons

Figure 2 shows Lf calculated with the four previously described different methodologies. The average Lf measured by EFOV (8.07±1.36 cm) was significantly shorter than the Lf values assessed by trigonometric equations A (9.98±2.12 cm, P<0.01) and B (8.57±1.59 cm, P=0.03). However, EFOV Lfs were not significantly different to Lfs estimated with the MLE method (8.40±1.68 cm, p=0.13). Significant correlations between Lfs (Fig 3 A) measured from EFOV

images and those calculated with MLE (r=0.81, CI=0.58-0.91, P<0.01) and Equation B (r=0.76, CI=0.50-0.89, P<0.01) extrapolation methods were observed, but no significant correlation was found between measured and estimated Lfs from Equation A (r=0.4, CI=-0.02-0.7, P=0.07). Bland-Altman plots (Fig 3B for absolute values) revealed average absolute biases in Lf compared with the EFOV technique of 1.91±2.1 cm from Equation A, 0.50±1.0 cm from Equation B and 0.33±1.0 cm from MLE.

Pennation angle and muscle thickness comparisons

Significant correlations between EFOV-derived and single image-derived PA (Fig 4A) and MT measurements (Fig 4B) were found (r=0.83, 95%CI: 0.68-0.90, P<0.01; r=0.88, 95%CI: 0.78-0.9, P<0.01, respectively). Bland-Altman plots (Fig 4) revealed an average absolute bias of -0.1±2.2 cm between single image-derived and EFOV-derived PA values, whereas an average absolute bias of -1.1±6 cm was found between single image-derived and EFOV-derived MT values.

Regional muscle architecture

Lf was significantly shorter distally than at the muscle mid-belly (Mid=8.07±1.36 vs. Distal=7.65±1.27, P=0.02). MT was smaller closer to the distal myotendinous junction compared with the muscle mid-belly (Mid=2.11±0.3 vs. Distal=1.87±0.3, P<0.01), as was PA but not significantly (Mid=14.87±4.07° vs. Distal=13.7±3.87°, P=0.30).

Discussion

The main finding of the present study was that BFlh Lf, as assessed by EFOV ultrasound imaging, was significantly overestimated on average with both of the trigonometric equations used here with a 5 cm ultrasound FOV. The most commonly used extrapolation method for BFlh Lf (i.e., trigonometric equation A - (9)) resulted in an Lf overestimation of almost ~2 cm compared with Lfs obtained from EFOV scans. The mean systematic bias in Lfs derived from Equation B and LE compared with EFOV scans was less at 0.5 cm and 0.33 cm, respectively. However, despite these average tendencies, all extrapolation methods led to both overestimations and underestimations of Lf compared with EFOV-derived Lfs (Fig 3), which suggests that the accuracy of all extrapolation methods is subject-specific and that the systematic error is not fixed between participants. This is problematic for assessing the relationship between BFlh Lf and hamstring muscle strain injury risk, as Lf from athlete X may be underestimated with the same extrapolation method that overestimates Lf from athlete Y, despite a mean systematic trend for Lf overestimation across participants. Similarly, changes in Lf pre- and post-intervention may simply be due to changes in the extrapolation error of Lf pre- and post-intervention, whereby small muscle architecture changes (i.e., systematic decreases in pennation angle) may result in a randomly underestimated Lf before training and a systematically overestimated Lf after training.

Test-retest repeatability: MLE and EFOV

Table 1 shows that MLE method presented very high repeatability for Lf and MT values (ICC=0.98 and 0.96, SEM=0.18 and 0.04, respectively) and high repeatability for PA measurements (ICC=0.85, SEM=0.5) (i.e., single operator = MVF). However, a clear advantage of the EFOV technique is that it allows for more of the fascicle and its surrounding structures

(i.e. aponeuroses) to be imaged compared with single ultrasound images, which likely improves the accuracy of muscle architecture measurements. We found a very high intra-day and intra-session reliability (for the single operator that acquired the scans – i.e., MVF) for Lfs measured from EFOV scans (ICC=0.96, r=0.96, SEM= 0.19 cm; Table 1). Pimenta and colleagues (7) previously reported similar intra-day repeatability values (ICC=0.95, r=0.95, SEM=0.19 cm) from what they described as the "non-linear EFOV technique", which consisted of acquiring panoramic scans of BFlh while attempting to stay in the fascicle plane (i.e., the same approach that was used in the present investigation). EFOV also showed high and very high intra-day and intra-session repeatability for PA and MT values, respectively (PA ICC=0.84, r=0.88, SEM=0.36 °; MT ICC=0.94, r=0.94, SEM=0.04 cm). Our data support the contention that the EFOV technique, once adequately practiced and optimized, can be considered as a strongly repeatable method for assessing the architecture of the BFlh muscle within the same session.

EFOV vs. extrapolation methods for BFlh Lf

The EFOV technique requires more operator training to scan muscles with heterogeneous architectures than conventional ultrasound imaging and is not as readily accessible as conventional B-mode ultrasound imaging. However, no study to date has assessed the validity of the most common extrapolation methods for estimating Lf of BFlh compared with the "non-linear EFOV technique". The main issues regarding BFlh Lf assessment at rest are that the BFlh has: i) a non-homogeneous fascicle arrangement along its muscle belly and ii) its fascicles are non-linear and may present a "S" shape (Fig 1), which has also been described by Pimenta and colleagues (7). A very similar fascicle arrangement has also been observed for the vastus medialis using freehand three-dimensional ultrasound imaging (16) and perhaps unsurprisingly

equation A was not able to reliably estimate Lf for this muscle either (9). Consequently, the extrapolation of the visible fascicle to obtain Lf is problematic within the BFlh and several factors can influence the degree of Lf over- or underestimation at rest, including 1) the subject's positioning, 2) where the fascicles are imaged from and which fascicles are analysed, 3) the transducer's scanning plane relative to the fascicle plane and level of pressure over the muscle belly, 4) the fascicle angle with respect to the intermediate aponeurosis, 5) the curvature of the fascicles and intermediate aponeurosis within the FOV (i.e., field of view), 6) and the curvature of fascicles and superficial aponeurosis outside the FOV. Points 5 and 6 likely result in the average underestimation of Lf from EFOV scans compared with extrapolation methods that we have observed here and the overestimation of VL Lf previously reported from the dual-probe technique (17) For example, a consistently concave fascicle within parallel aponeuroses would result in an underestimation of Lf with a straight line (e.g. VL) and a concave and convex fascicle (e.g. BFlh) would result in both underestimation and overestimation of Lf with a straight line. The under- or overestimation of Lf with a straight line is dependent on whether the visible concave curvature is greater (underestimation) or less (overestimation) than the non-visible convex curvature. The average trend we observed suggests that BFlh fascicles likely have more convex than concave curvature at the distal vs. mid-muscle belly, but this is not the case in every individual and might be influenced by slight differences in probe placement. Below we have provided some recommendations to help determine more accurate Lfs using each extrapolation method that we compared with EFOV ultrasound scans.

Trigonometric Equation A

Equation A is a trigonometric formula that requires the input of three muscle architecture variables (MT, PA and γ = angle between aponeuroses) and, apart from the manual digitization of pennation angles, does not involve any further direct manual assessment of the visible portions of fascicles (18). This extrapolation method may be suitable for estimating Lf in muscles that present a relatively linear fascicle arrangement, such as the GM, or a consistent fascicle curvature, such as the VL, but it is clearly not suitable for the vastus medialis due to its regionally variable and substantial fascicle curvature (9). Not only does this equation neglect fascicle curvature, but it does not take into account a) possible aponeurosis curvature outside the FOV (which may subsequently impact the MT and aponeurosis angle inputs) (6) or b) the potential bias introduced by non-parallel alignment of the aponeuroses due to improper probe alignment or muscle architecture heterogeneity. Indeed, aponeurosis angle can markedly influence the estimation of Lf (e.g. one subject, later excluded from our comparisons, presented a 24.29 cm Lf estimated using equation A, where γ was 6.40°, PA was 11.12° and MT was 1.97 cm). However, even when care was taken to ensure that the superficial and intermediate aponeuroses were "as parallel as possible", in some cases this could not be achieved. For this reason, and for the sake of method comparisons for estimating Lf, we decided to only include volunteers that presented a $\gamma < 4°$ (n=22 out of 37) in order to minimize this source of bias. Despite this and other technical precautions outlined in the methods, Equation A still resulted in a mean extrapolation of 58.3% of the Lf.

As previously mentioned, both trigonometric equations resulted in a significant systematic overestimation of Lf. However, for equation A, underestimation of Lf was also observed in 5 out of 22 participants. This is likely to be because of differences in PA between participants. For example, if we consider for simplicity two muscles that have completely parallel aponeuroses (γ=0 °) and the same MT (2.1 cm, average of the present study), but have PAs that are 5° different ($muscle_a$=10°, considered as a lower PA compared with the average of the present study, vs. $muscle_b$= 15°), Lf_a will be 12 cm and Lf_b will be 8.1 cm as calculated by equation A. This ~4 cm difference because of PA differences could be real and physiologically-plausible (e.g. due to training-related adaptations) or due to differences in transducer pressure or transducer alignment even if the transducer placement is standardised. To back this up with actual data, we observed that, in 4 athletes with PA values ranging between 13.5-18.9° (MT range=1.84-2.69 cm), equation A resulted in an underestimation of Lf compared with EFOV scans (range= 0.25-1.03 cm). Conversely, in 10 athletes who had PA values ranging between 10.3-13.4° (MT range=1.64-2.25 cm), equation A resulted in an overestimation of Lf compared with EFOV scans (range= 0.39-6.72 cm). However, despite these trends in PA for predicting under- or overestimation of Lf, it should be noted that there are exceptions because of BFlh's heterogeneous muscle architecture (e.g. one athlete with a PA of 20° and MT of 2.3 cm did not have an underestimation of Lf from equation A when compared with EFOV-derived Lf, even though the PA was higher than the study's average). This further reinforces the idea that the systematic error in Lf estimates from one extrapolation method is not fixed between participants and may be affected by transducer-related or training-related PA changes between testing sessions.

Trigonometric equation B and MLE

Equation B estimated Lf for approximately ~52% of Lf. Equation B is another trigonometric formula that requires 3 inputs (L = length of visible portion of fascicles, h = distance between superficial aponeurosis and the last visible point of the fascicle, and β = the angle formed between the linear projections of the superficial aponeurosis and fascicle of interest). The most noteworthy difference between trigonometric methods is that, while Equation A does not take into account the curvature of the visible part of the fascicle, equation B accounts for fascicle curvature and the slope of the linear projection of the fascicle is related to the most distal visible point of the fascicle rather than the most proximal visible point of the fascicle.

In this study, despite a consistently smaller Lf overestimation with Equation B compared with Equation A, EFOV Lf values were still significantly shorter than those obtained with Equation B ($p = 0.03$), supporting the previous work by Pimenta et al. (7). Nevertheless, in 8 athletes out of 22, Equation B resulted instead in an underestimation of Lf values (range= 0.21-1.22 cm), whereas in 13 athletes Equation B presented an overestimation of Lf compared to EFOV scans (range=0.51-2.22 cm). Once again, these observations reinforce the idea that the systematic error in Lf estimates is not fixed between participants, and in the case of Equation B, this is most likely due to the curvature of fascicles and the superficial aponeurosis outside of the FOV.

Lf derived from EFOV and MLE were not significantly different ($p=0.13$) and ~49% of the Lf was estimated from the MLE method. Thus, the accuracy of extrapolation methods with respect to the EFOV technique seems to be dependent on the length of the fascicle that is visible and whether it is digitised or not.

Regional differences in BFlh muscle architecture

While the primary aim of the present investigation was to compare Lfs derived from different methodologies from a clearly defined ROI (mid-belly of BFlh), regional differences in BFlh architecture (Mid vs. Distal muscle sites) were also found for all three muscle architectural parameters from the EFOV scans, which supports previous reports (13, 14, 19, 20). MT was smaller closer to the distal myotendinous junction compared with the muscle mid-belly (2.11±0.3 vs. 1.87±0.3), as was PA (14.87±4.07° vs. 13.7±3.87°). In addition, Lf was shorter distally (Mid = 8.07±1.36 vs. Distal = 7.65±1.27). These data once again indicate the importance of keeping the same ROI over time for ultrasound imaging, as errors in probe placement could strongly influence the muscle architecture outcomes. Furthermore, it is important to note that, when using the EFOV technique to describe Lf changes over time in response to loading or unloading, fascicles from different muscle sites should not be averaged, as this could reduce the magnitude of muscle architecture changes at specific muscle sites.

Physiological perspective

In training scenarios, distinctive adaptations in BFlh muscle architecture have been reported over training periods of 2 to 8 weeks (1, 10, 21–26) and 12 weeks (27). The magnitudes of Lf increase have been reported to range from 13-24% for Nordic hamstring exercise training and 34% following eccentrically-biased hamstring curl training (10), whereas 5-12% reductions in Lf following isometric or concentric training have been found (2). However, a very recent study, which employed EFOV modality, showed only modest increases in BFlh Lf (4.5 to 4.8%) in response to 6 weeks of NHE and modified stiff-leg deadlift (15). Moreover, for the VL muscle (which has a validated extrapolation method to estimate Lf), the magnitudes of change over

similar training periods (4 weeks) in response to concentric only and eccentric only resistance training were much smaller (~5% - however a 10 cm linear transducer was implemented and linear extrapolation was only used when needed) (28). Even after 8 to 10 weeks of eccentric-only training, VL Lf was not increased by more than 10.4-12% (29, 30). Another study that employed isokinetic concentric-only and eccentric-only training did not observe an increase in VL Lf of more than ~12% over the 5-weeks of training (a 5 cm transducer and Equation A extrapolation method were employed) (18). Thus, (although the latter data are not from the BFlh), it is still pertinent to question why the magnitude of Lf changes found in previous studies of the BFlh with extrapolation methods that are not yet validated in this muscle are so much greater than the training-induced Lf changes reported in VL.

A further proof that BFlh Lf estimations may be problematic can be found in *Ex vivo* studies. Cadaver-based values still represent the most reliable source for comparison of US-assessed Lfs from different muscles, although some limitations remain (i.e., pre-mortem age, health status of patients, fixation artefacts) (31). Muscles with relatively shorter fascicles and more homogenous architectures than BFlh (i.e., GM, TA) show good agreement in Lf measurements between cadaveric reports and ultrasound-based assessments. However, this is not the case for the majority of BFlh Lf estimates. Cadaveric reports of mean BFlh Lfs range from 6.22 to 9.76 cm (19, 31–36). However, previous *in vivo* studies that have used extrapolation methods and the EFOV technique for Lf assessment have found mean pre-intervention values of between 5.73 and 11.94 cm (1, 3, 7, 10, 22–26, 37) (Table 2). It could be argued that this substantial Lf variability may be due to the choice of extrapolation technique, as similar field of view linear transducers were used for most of the aforementioned studies (from ~4.1 to 4.7 cm in eight

studies (1, 3, 10, 22–26), 6 cm in two studies (7, 37) and 8 cm in the two remaining studies (35, 38)). Note that the studies that employed equation A to estimate Lf showed the highest range (from 8.17 to 11.94 cm) (1, 3, 7, 10, 22–26, 37) and that we also found this method resulted in the longest estimated Lf on average. Moreover, following Nordic hamstring exercise interventions, mean Lf estimates can be found up to 13.4 cm (1), which is 3.66 cm greater than the largest reported cadaveric value (34). It is worth highlighting that studies that have used the EFOV technique provided Lf values in the range of the cadaveric observations and closer to the Lf data obtained in the present investigation (range = 7.69 to 9.1 cm) (7, 14, 15, 20).

Based on the data from this study, we caution against using extrapolation methods to estimate BFlh Lf, as the level of over- or underestimation is not consistent across participants and thus the influence of the extrapolation method on the calculated Lf is unknown. Since the extrapolation equations strongly depend on muscle architecture-related input measures, such as fascicle and aponeurosis orientation, MT and PA. This can become particularly problematic when assessing the magnitudes of training effects, since training-induced changes in muscle architecture (such as PA) may randomly bias the estimated changes of BFlh Lf between baseline and follow-up. Lastly, as equation A results in the largest errors in Lf and equation B still presents values of Lf which are significantly different to EFOV-derived ones, we recommend the use of MLE on the largest field of view possible if only conventional ultrasound imaging is available. However, even though MLE shows the best agreement with EFOV-derived Lf values, this investigation did not investigate the accuracy of the MLE method in quantifying architectural changes compared with EFOV. Thus, we cannot be sure that this agreement would remain if the muscle was subject to loading or unloading and in order to understand the accuracy of MLE (e.g. when EFOV

technique cannot be implemented), the use of dual probe array (17) or multiple scan sites should be further investigated on BFlh.

Study limitations

Although the EFOV technique offers advantages compared with conventional ultrasound imaging, it should not be considered as the "gold standard" for the assessment of Lf as it has some important limitations. The EFOV technique relies on texture mapping algorithms to merge sequences of images collected during real-time scanning to reconstruct large composite images. As the transducer is moved along the skin surface and along the fascicle plane, successive frames are recorded and stitched together to obtain a panoramic image. However, there are inherent difficulties in scanning large regions with variable muscle architecture and stitching errors between images could be made by temporary transducer misalignment or differences in transducer pressure, as seen in the "linear" EFOV scans shown by Pimenta and colleagues (7). Nevertheless, when care is taken in order to stay in the fascicle plane during scanning, very high repeatability has been observed for BFlh muscle parameters in previous studies (7, 14) and in our present work. Thus, EFOV can provide important insights into a muscle's regional and global architecture and can be used to quantify how this might change following specific interventions. Alternatively, freehand three-dimensional ultrasound (39) or diffusion tensor imaging could be employed to provide more accurate estimates of BFlh Lf (40). DTI requires further investigation due to a previously reported poor absolute reliability (SEM = 1.27 cm (14%), although ultrasound-derived Lf values were estimated by Equation A (41).

Conclusions

The present data demonstrate that the linear extrapolation of visible fascicles from single 5 cm FOV ultrasound images generally results in overestimations of BFlh Lf when compared with EFOV scans. Although Lfs estimated with the same extrapolation method are highly reliable within the same session, the differences in Lf between each extrapolation method and the EFOV scans are not consistent between individuals, which suggests that the extrapolation errors cannot be predicted. These findings raise a call for caution for physiologists, biomechanists, strength and conditioning researchers and sports medicine experts when investigating training adaptations, muscle models, and injury prevention strategies within the BFlh. Further technique developments (e.g., freehand three-dimensional ultrasound imaging) should be implemented in the search for a gold standard for the assessment of BFlh Lf, so that the third dimension of muscle architecture can be taken into account.

Acknowledgements

The authors would like to thank Swiss Ski and Balgrist foundation stitftung for the financial support for the present study.

Conflict of interests

The authors declare the non-presence of any conflict of interests. The results of the present study do not constitute endorsement by ACSM. The results of the present study are presented clearly, honestly, without fabrication, falsification or inappropriate data manipulation.

References

1. Timmins RG, Shield AJ, Williams MD, Lorenzen C, Opar DA. Biceps Femoris Long Head Architecture. *Med Sci Sport Exerc*. 2015;47(5):905–13.
2. Bourne MN, Timmins RG, Opar DA, et al. An Evidence-Based Framework for Strengthening Exercises to Prevent Hamstring Injury. *Sport Med*. 2018;48(2):251–67.
3. Guex K, Degache F, Morisod C, Sailly M, Millet GP. Hamstring Architectural and Functional Adaptations Following Long vs. Short Muscle Length Eccentric Training. *Front Physiol*. 2016;7:340.
4. Fiorentino NM, Blemker SS. Musculotendon variability influences tissue strains experienced by the biceps femoris long head muscle during high-speed running. *J Biomech*. 2014;47(13):3325–33.
5. Timmins RG, Shield AJ, Williams MD, Lorenzen C, Opar DA. Architectural adaptations of muscle to training and injury: a narrative review outlining the contributions by fascicle length, pennation angle and muscle thickness. *Br J Sports Med*. 2016;50(23):1467–72.
6. Franchi M V., Raiteri BJ, Longo S, Sinha S, Narici M V., Csapo R. Muscle Architecture Assessment: Strengths, Shortcomings and New Frontiers of in Vivo Imaging Techniques [Internet]. *Ultrasound Med Biol*. 2018 [cited 2018 Sep 21]; available from: https://www.sciencedirect.com/science/article/pii/S0301562918302862. doi:10.1016/J.ULTRASMEDBIO.2018.07.010.
7. Pimenta R, Blazevich AJ, Freitas SR. Biceps Femoris Long-Head Architecture Assessed Using Different Sonographic Techniques. *Med Sci Sport Exerc*. 2018;50(12):2584–94.
8. Ando R, Taniguchi K, Saito A, Fujimiya M, Katayose M, Akima H. Validity of fascicle length estimation in the vastus lateralis and vastus intermedius using ultrasonography. *J*

Electromyogr Kinesiol. 2014;24(2):214–20.

9. Blazevich AJ, Gill ND, Zhou S. Intra- and intermuscular variation in human quadriceps femoris architecture assessed in vivo. *J Anat*. 2006;209(3):289–310.
10. Potier TG, Alexander CM, Seynnes OR. Effects of eccentric strength training on biceps femoris muscle architecture and knee joint range of movement. *Eur J Appl Physiol*. 2009;105(6):939–44.
11. Finni T, Ikegaw S, Lepola V, Komi P. In vivo behavior of vastus lateralis muscle during dynamic performances. *Eur J Sport Sci*. 2001;1(1):1–13.
12. Noorkoiv M, Stavnsbo A, Aagaard P, Blazevich AJ. In vivo assessment of muscle fascicle length by extended field-of-view ultrasonography. *J Appl Physiol*. 2010;109(6):1974–9.
13. Bennett HJ, Rider PM, Domire ZJ, DeVita P, Kulas AS. Heterogeneous fascicle behavior within the biceps femoris long head at different muscle activation levels. *J Biomech*. 2014;47(12):3050–5.
14. Seymore KD, Domire ZJ, DeVita P, Rider PM, Kulas AS. The effect of Nordic hamstring strength training on muscle architecture, stiffness, and strength. *Eur J Appl Physiol*. 2017;117(5):943–53.
15. Lacome M, Avrillon S, Cholley Y, Simpson BM, Guilhem G, Buchheit M. Hamstring Eccentric Strengthening Program: Does Training Volume Matter? *Int J Sports Physiol Perform*. 2019;1–27.
16. Hug F, Goupille C, Baum D, Raiteri BJ, Hodges PW, Tucker K. Nature of the coupling between neural drive and force-generating capacity in the human quadriceps muscle. *Proc R Soc B Biol Sci*. 2015;282(1819):20151908.
17. Brennan SF, Cresswell AG, Farris DJ, Lichtwark GA. In vivo fascicle length measurements via B-mode ultrasound imaging with single vs dual transducer arrangements. *J Biomech*.

2017;64:240–4.

18. Blazevich AJ, Cannavan D, Coleman DR, Horne S. Influence of concentric and eccentric resistance training on architectural adaptation in human quadriceps muscles. *J Appl Physiol*. 2007;103(5):1565–75.

19. Kellis E, Galanis N, Natsis K, Kapetanos G. Muscle architecture variations along the human semitendinosus and biceps femoris (long head) length. *J Electromyogr Kinesiol*. 2010;20(6):1237–43.

20. Kellis E, Galanis N, Natsis K, Kapetanos G. Validity of architectural properties of the hamstring muscles: Correlation of ultrasound findings with cadaveric dissection. *J Biomech*. 2009;42(15):2549–54.

21. Bourne MN, Duhig SJ, Timmins RG, et al. Impact of the Nordic hamstring and hip extension exercises on hamstring architecture and morphology: implications for injury prevention. *Br J Sports Med*. 2017;51(5):469–77.

22. Ribeiro-Alvares JB, Marques VB, Vaz MA, Baroni BM. Four Weeks of Nordic Hamstring Exercise Reduce Muscle Injury Risk Factors in Young Adults. *J strength Cond Res*. 2018;32(5):1254–62.

23. Alonso-Fernandez D, Docampo-Blanco P, Martinez-Fernandez J. Changes in muscle architecture of biceps femoris induced by eccentric strength training with nordic hamstring exercise. *Scand J Med Sci Sports*. 2018;28(1):88–94.

24. Timmins RG, Ruddy JD, Presland J, et al. Architectural Changes of the Biceps Femoris Long Head after Concentric or Eccentric Training. *Med Sci Sport Exerc*. 2016;48(3):499–508.

25. Duhig SJ, Bourne MN, Buhmann RL, et al. Effect of concentric and eccentric hamstring training on sprint recovery, strength and muscle architecture in inexperienced athletes [Internet]. *J Sci Med Sport*. 2019 [cited 2019 Mar 21]; available from:

http://www.ncbi.nlm.nih.gov/pubmed/30772189. doi:10.1016/j.jsams.2019.01.010.

26. Pollard CW, Opar DA, Williams MD, Bourne MN, Timmins RG. Razor hamstring curl and Nordic hamstring exercise architectural adaptations: Impact of exercise selection and intensity. *Scand J Med Sci Sports*. 2019;sms.13381.

27. Lovell R, Knox M, Weston M, Siegler JC, Brennan S, Marshall PWM. Hamstring injury prevention in soccer: Before or after training? *Scand J Med Sci Sports*. 2018;28(2):658–66.

28. Franchi M V, Wilkinson DJ, Quinlan JI, et al. Early structural remodeling and deuterium oxide-derived protein metabolic responses to eccentric and concentric loading in human skeletal muscle [Internet]. *Physiol Rep*. 2015; available from: http://www.scopus.com/inward/record.url?eid=2-s2.0-84960120595&partnerID=MN8TOARS. doi:10.14814/phy2.12593.

29. Franchi M V, Atherton PJ, Reeves ND, et al. Architectural, functional and molecular responses to concentric and eccentric loading in human skeletal muscle. *Acta Physiol (Oxf)*. 2014;210(3):642–54.

30. Franchi MV, Ruoss S, Valdivieso P, et al. Regional regulation of focal adhesion kinase after concentric and eccentric loading is related to remodelling of human skeletal muscle [Internet]. *Acta Physiol*. 2018; doi:10.1111/apha.13056.

31. Wickiewicz TL, Roy RR, Powell PL, Edgerton VR. Muscle architecture of the human lower limb. *Clin Orthop Relat Res*. 1983;(179):275–83.

32. Friederich JA, Brand RA. Muscle fiber architecture in the human lower limb. *J Biomech*. 1990;

33. Woodley SJ, Mercer SR. Hamstring Muscles: Architecture and Innervation. *Cells Tissues Organs*. 2005;179(3):125–41.

34. Ward SR, Eng CM, Smallwood LH, Lieber RL. Are current measurements of lower extremity muscle architecture accurate? *Clin Orthop Relat Res*. 2009;467(4):1074–82.

35. Chleboun GS, France AR, Crill MT, Braddock HK, Howell JN. In vivo Measurement of Fascicle Length and Pennation Angle of the Human Biceps femoris Muscle. *Cells Tissues Organs*. 2001;169(4):401–9.

36. Ruggiero M, Cless D, Infantolino B. Upper and Lower Limb Muscle Architecture of a 104 Year-Old Cadaver. *PLoS One*. 2016;11(12):e0162963.

37. Freitas SR, Marmeleira J, Valamatos MJ, Blazevich A, Mil-Homens P. Ultrasonographic Measurement of the Biceps Femoris Long-Head Muscle Architecture. *J Ultrasound Med*. 2018;37(4):977–86.

38. e Lima KMM, Carneiro SP, de S. Alves D, Peixinho CC, de Oliveira LF. Assessment of Muscle Architecture of the Biceps Femoris and Vastus Lateralis by Ultrasound After a Chronic Stretching Program. *Clin J Sport Med*. 2015;25(1):55–60.

39. Raiteri BJ, Cresswell AG, Lichtwark GA. Three-dimensional geometrical changes of the human tibialis anterior muscle and its central aponeurosis measured with three-dimensional ultrasound during isometric contractions. *PeerJ*. 2016;4:e2260.

40. Bolsterlee B, Veeger HEJ (DirkJan), van der Helm FCT, Gandevia SC, Herbert RD. Comparison of measurements of medial gastrocnemius architectural parameters from ultrasound and diffusion tensor images. *J Biomech*. 2015;48(6):1133–40.

41. Behan FP, Vermeulen R, Smith T, et al. Poor agreement between ultrasound and inbuilt diffusion tensor MRI measures of biceps femoris long head fascicle length. *Transl Sport Med*. 2019;2(2):58–63.

FIGURE CAPTIONS

Figure 1. ROIs and transducer positioning for all ultrasound scans. A = On top, the ultrasound imaging path marked along the longitudinal plane is displayed, then below three photographs (from distal to proximal) captured during an EFOV scan acquisition are shown (position 2 = 50% of femur length, thus the single ultrasound image scan site); B = representative scans of a representative athlete: the same ROI was identified between the EFOV scan and the single ultrasound image for further Lf analysis. The same Lf digitization outside the field of view has been copied from the EFOV scan onto the single ultrasound image (on top): the red dotted lines show the discrepancy in the fascicle length between EFOV and single image when the curvature of the superficial aponeurosis is not accounted for, resulting, in the present case, in overestimation of Lf with a restricted field of view.

Figure 2. Comparison of Lf values assessed by extrapolation methods and EFOV scans (mean ± S.D.). *=P<0.05 **= P<0.01

Figure 3. Agreement of Lf measurements between EFOV and extrapolation methods (LE, equation A and equation B): linear regressions (A) and Bland-Altman analyses (B) showing absolute differences with respect to the average Lf obtained between methodologies. ULOA = upper limit of agreement, LLOA = lower limit of agreement.

Figure 4. Agreement of PA and MT measurements between EFOV and single ultrasound imaging: linear regressions (A) and Bland-Altman analyses (B) showing absolute differences with respect to the average PA and MT obtained between methodologies. ULOA = upper limit of agreement, LLOA = lower limit of agreement.

Figure 1

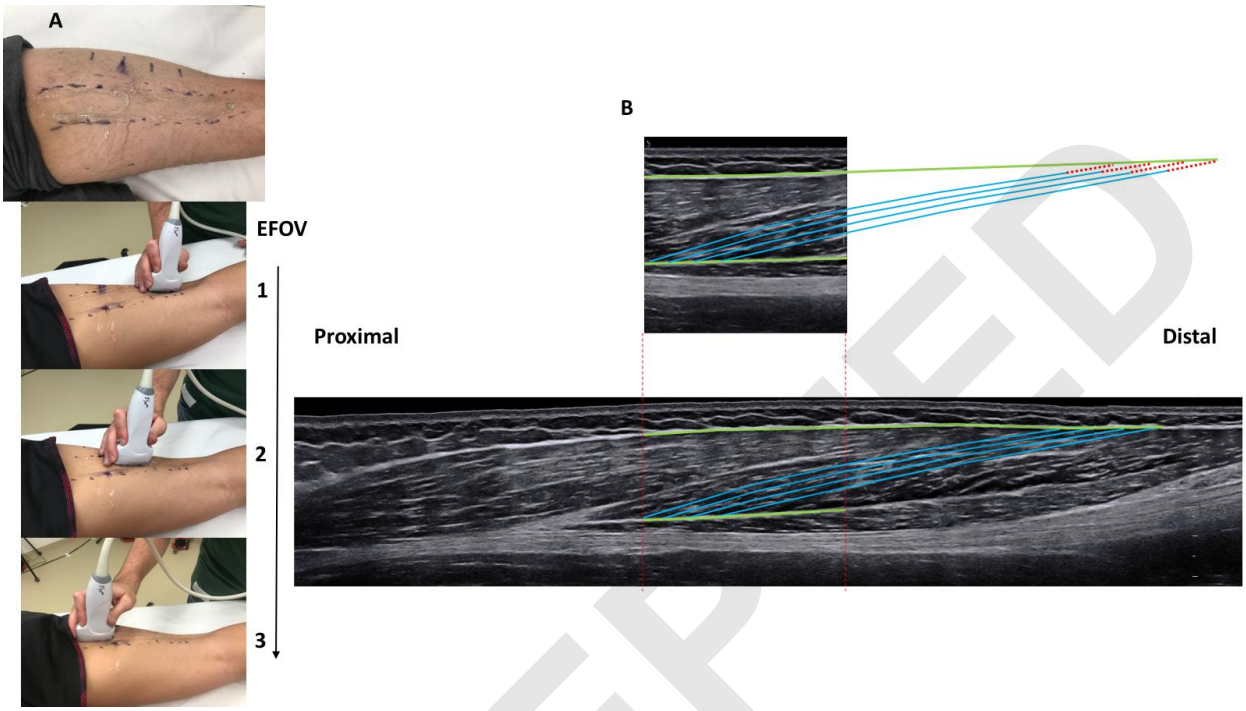

Figure 2

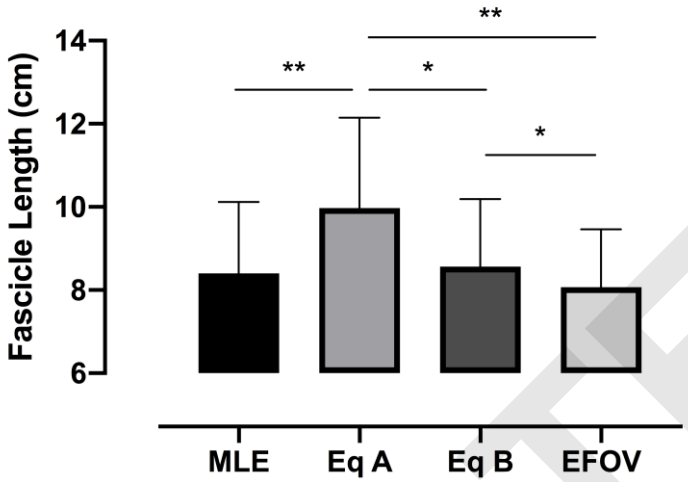

Figure 3

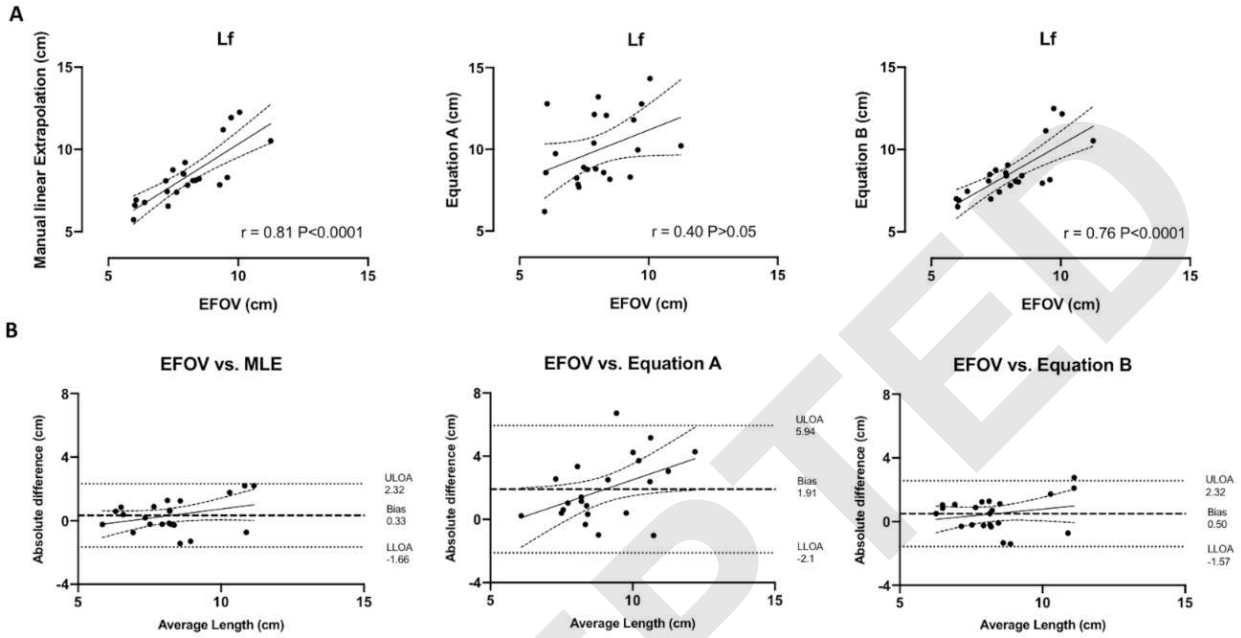

Figure 4

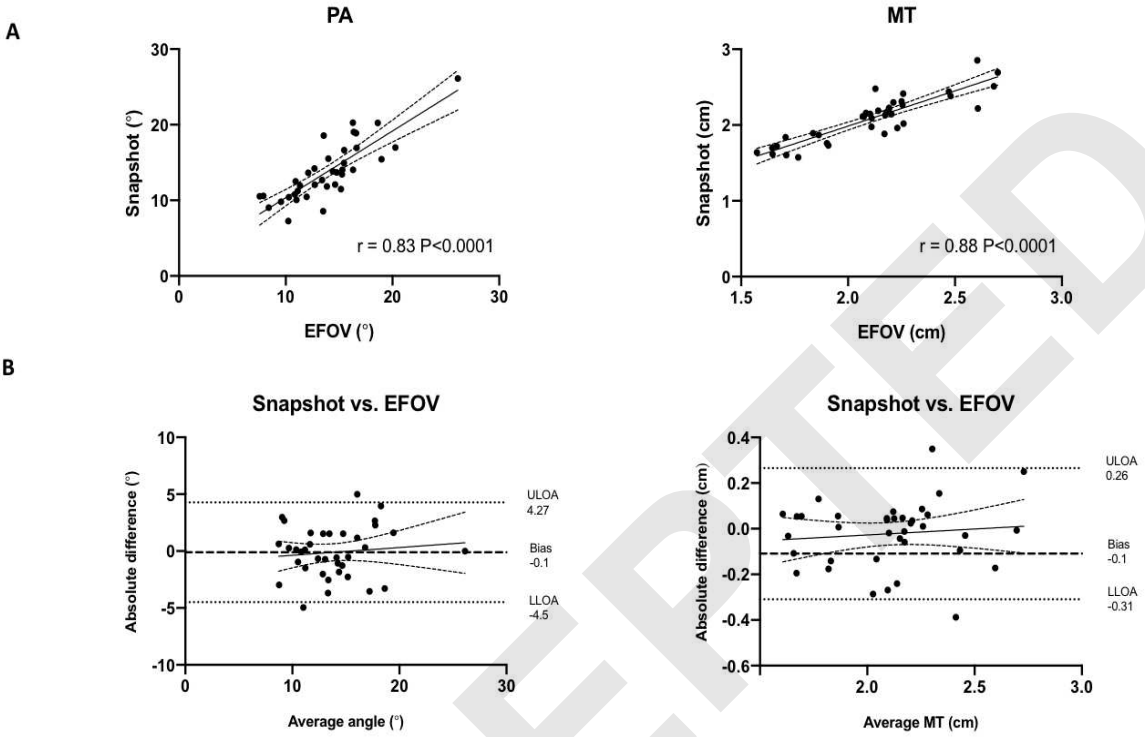

Parameter	Technique	Measure1	Measure2	$ICC_{3,k}$ (95% CI)	*r*	SEM
Lf (cm)	US snapshot (LE)	8.93±0.99	9.04±0.8	0.98 (0.96-0.99)	0.98	0.18
	EFOV	8.60±0.73	8.73±0.75	0.96 (0.91-0.98)	0.96	0.19
PA (°)	US snapshot	13.73±3.74	14.3±3.38	0.85 (0.69-0.93)	0.85	0.5
	EFOV	10.1±2.64	10.62±2.06	0.84 (0.73-0.95)	0.88	0.36
MT (cm)	US snapshot	2.12±0.3	2.12±0.31	0.96 (0.92-0.98)	0.96	0.04
	EFOV	2.08±0.26	2.07±0.28	0.94 (0.88-0.97)	0.94	0.04

Table 1. Intra-session repeatability for muscle architecture parameters measured from either a single 5 cm field of view ultrasound image or the non-linear EFOV technique (n=6). Measure 1 and Measure 2 represent the average values for the analyses carried out on multiple fascicles (total number=4) or from multiple sites for thickness values (total number n=5) within the same ultrasound image.

ICC = intraclass correlation coefficient, *r* = Pearson's coefficient, SEM = standard error of the mean.

Study	US technique	Transducer length	ROI	MT (cm)	PA (°)	Lf (cm)	Lf extrapolation method
Chleboun et al. 2001 (*)	Multiple image stitching (3-7 images)	8 cm	From most distal point upwards	-	13.8± 3.1	8.8±1.8	No Extrapolation
Potier et al. 2009	Single ultrasound image	4.1 cm	Between mid-muscle belly and distal end	-	Range 13.9-14.8 (16.6-17.1 after RET)	Range 5.73-5.9 (6.68-7.88 after RET)	Linear Extrapolation
Timmins et al. 2015	Single ultrasound image	4.7 cm	Mid-point of Ischial tuberosity and knee-joint fold	Range 2.34-2.45	Range 12.81-12.94	Range 10.7-11.94	Trigonometric Equation A
E Lima et al. 2015	Single ultrasound image	8 cm	Mid-point of greater trochanter and popliteal crease	Range 2.26-2.53 (2.34-2.59 after intervention)[#]	Range 14.89-16.66 (15.22-16.78 after intervention)[#]	Range 8.13-8.77 (7.83-8.26 after intervention)[#]	Linear Extrapolation
Kellis et al. 2009 (*)	EFOV (non-linear)	Not specified	Whole muscle *(average of values at 4 muscle sites, from distal to proximal)*	1.41±0.37	13.88±2.76	8.04±1.66	No Extrapolation
Timmins et al. 2016	Single ultrasound image	4.7 cm	Mid-point of Ischial tuberosity and knee-joint fold	Range 2.54-2.69	Range 12.57-13.52	Range 11.53-11.71	Trigonometric Equation A

				(2.68-2.91 after RET)	(12.50-15.1 after RET)	(10.33-13.42 after RET)	
Guex et al. 2016	Single ultrasound image	4.2 cm	Middle belly of BFlh (longitudinal plane position not specified)	-	Range 14.6-15 (13.8.-14.9 after RET)	Range 8.2-8.41 (8.82-8.94 after RET)	Linear Extrapolation
Alonso-Fernandez et al. 2017	Single ultrasound image	4.7 cm	Mid-point of Ischial tuberosity and knee-joint fold	2.09±0.47 (2.25±0.39 after RET)	14.74±1.91 (12.55±1.34 after RET)	8.17±1.83 (10.12±1.85 after RET)	Trigonometric Equation A
Seymore et al. 2017	EFOV (non-linear)	Not specified	Whole muscle *(average of distal, mid and proximal values)*	-	Range 13.1-13.6 (13.4-14.9 after RET)	Range 8.19-8.96 (8.01-9.07 after RET)	No Extrapolation
Freitas et al. 2017	Single ultrasound image	6 cm	Mid- point between distal and proximal insertions	Range 1.98-2.04	Range 12.5-12.7	Range 9.64-9.99	Trigonometric Equation B
Riberio-Alvares et al. 2018	Single ultrasound image	4 cm	Mid-point of Ischial tuberosity and superior border of fibular head	Range 2.02-2.05 (2.04-2.07 after RET)	Range 12.77-14 (11.64-12.64 after RET)	Range 8.36-9.4 (9.59-10.18 after RET)	Trigonometric Equation A
Pimenta al. 2018	Single ultrasound image / EFOV	6 cm	Mid- point between distal and proximal insertions	Range 2.41-2.44 (2.41-2.43 for	Range 16.4-16.6 (18-18.1 for	Range 8.41-8.58 (7.69-7.81	Trigonometric Equation B / No extrapolation

	(non-linear)			EVOF)	EVOF)	for EVOF)	for EFOV scans
Pollard et al. 2019	Single ultrasound image	4.7 cm	Mid-point of Ischial tuberosity and knee-joint fold	Range 2.36-2.56 (2.43-2.67 after RET)	Range 14.87-16 (13.34-15.88 after RET)	Range 9.76-9.85 (9.71-11.42 after RET)	Trigonometric Equation A
Duhig et al. 2019	Single ultrasound image	4.7 cm	Mid-point of Ischial tuberosity and knee-joint fold	Range 2.49-2.55 (2.66-2.68 after RET)	Range 14.16-14.18 (13.39-15.91 after RET)	Range 10.22-10.39 (9.73-11.62 after RET)	Trigonometric Equation A

Table 2. Summary of studies that assessed BFlh tLf by EFOV, equation A, equation B and LE.

Data not included for Presland et al. 2018, Bourne et al. 2017 or Bennet et al. 2014 as no absolute values were presented. (*) = cadaveric samples RET = resistance exercise training, # = stretching intervention.